

Resolution and Noise Properties of Linear Phase-Constrained Partial Fourier Reconstruction

J. P. HALDAR¹, K. SAKAIE², AND Z-P. LIANG¹

¹BECKMAN INSTITUTE, ELECTRICAL AND COMPUTER ENGINEERING, UNIVERSITY OF ILLINOIS AT URBANA-CHAMPAIGN, URBANA, IL, UNITED STATES, ²CLEVELAND CLINIC, CLEVELAND, OH, UNITED STATES

INTRODUCTION

Phase-constrained partial Fourier (PF) reconstruction techniques employ prior knowledge of the image phase to significantly reduce k -space sampling requirements, and have typically been evaluated either using empirical results or qualitatively through analogy to the context of smooth phase and infinite sampling [1,2]. In this work, we show that the resolution and noise properties of linear PF reconstruction can be characterized in terms of *spatial response functions* (SRFs) and *interference response functions* (IRFs). These characterizations can be used to simplify the selection of reconstruction parameters.

THEORY

Data collection in standard MRI can be modeled as Eq. (1), where $\rho(\mathbf{x})$ is the desired image, and the η_m represent white Gaussian noise perturbations with variance σ^2 . In addition to the data, we have prior knowledge that $\rho(\mathbf{x})$ approximately has phase $\varphi(\mathbf{x})$, such that the phase corrected image $\rho_p(\mathbf{x})$ defined in Eq. (2) is almost purely real. In linear PF reconstruction methods (including homodyne reconstruction [3] and matrix inversion methods [4,5]), an estimate of $\rho_p(\mathbf{x})$ is computed as a linear combination of the acquired data as in Eqs. (3) and (4), where $a_m(\mathbf{y})$, $b_m(\mathbf{y})$, $c_m(\mathbf{y})$, and $d_m(\mathbf{y})$ are the (spatially-varying) real-valued linear reconstruction coefficients. Using Eqs. (1) and (2), Eq. (3) can be rewritten as Eq. (5) in terms of the true image, the SRF, the IRF, and a noise perturbation. The SRF, IRF, and noise perturbation terms are defined in Eqs. (6)-(8). Similar expressions exist for the SRF and IRF for $\text{imag}[\rho_{p,\text{recon}}(\mathbf{y})]$ in terms of the $c_m(\mathbf{y})$, and $d_m(\mathbf{y})$ coefficients.

Equation (5) describes the relationship between the reconstructed image and the true underlying image, which is an important characterization to have. The SRF can be used to quantify the resolution of the image, while the IRF can be used to assess the possible perturbation due to phase inconsistency.

RESULTS

We have observed that in the presence of smooth phase variation, the SRFs and IRFs for standard linear PF reconstruction methods are fairly consistent throughout the FOV. Figure 1 shows a simulated example (5/8th PF acquisition, with smoothly-varying phase constraints) where homodyne reconstruction [3] and standard Tikhonov-regularized PF reconstruction [4,5] SRFs and IRFs are compared with a regularized PF reconstruction that incorporates a quadratic penalty on the finite differences of the image to promote spatial smoothness. Also see Fig. 2.

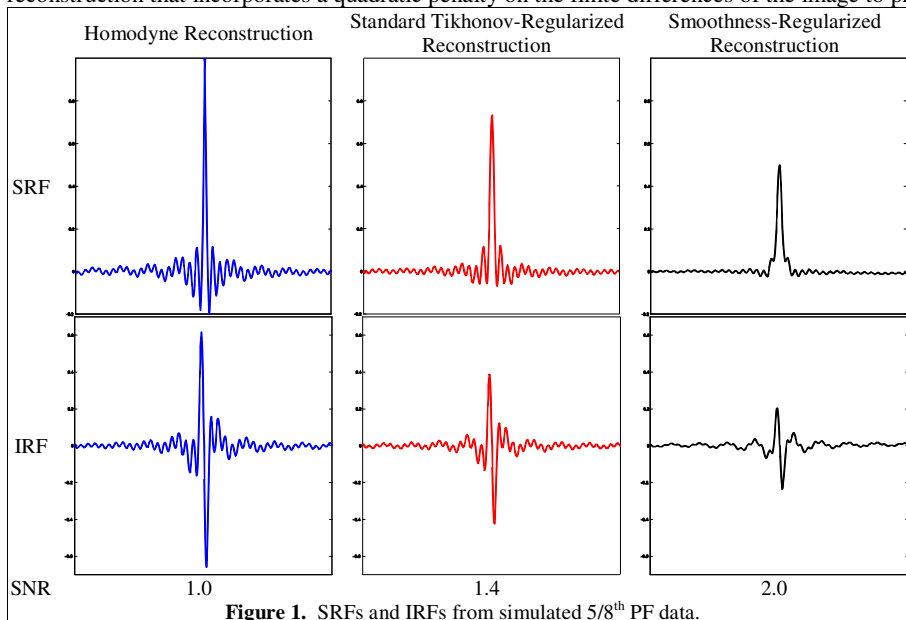


Figure 1. SRFs and IRFs from simulated 5/8th PF data.

The regularization parameters were chosen to achieve a desired SNR/resolution trade-off. The achievable SNR improvement for standard Tikhonov regularization seems limited, while it is unlimited for smoothness regularization. Use of the smoothness prior has an effect similar to apodization, where truncation artifacts are reduced, the SNR improves, and the resolution is slightly degraded. Characterization in terms of the SRF provides a new mechanism for selecting regularization parameters, and provides more insight than previous methods which use the L-curve [5].

REFERENCES

- [1] Z.-P. Liang, *Rev Magn Reson Med* 1991;4:67-185. [3] D. Noll, *IEEE Trans Med Imag* 1991;10:154-163. [5] W. Hoge, *IEEE ISBI* 2007; 1012-1015.
 [2] G. McGibney, *Magn Reson Med* 1993;30:51-59. [4] M. Bydder, *Magn Reson Med* 2005;53:1393-1401. [6] J. Haldar, *ISMRM* 2008; 141.

Equations
(1) $d(\mathbf{k}_m) = \int \rho(\mathbf{x}) \exp(-i2\pi \mathbf{k}_m \cdot \mathbf{x}) d\mathbf{x} + \eta_m, m = 1, \dots, M$
(2) $\rho_p(\mathbf{x}) = \rho(\mathbf{x}) \exp(-i \varphi(\mathbf{x}))$
(3) $\text{real}[\rho_{p,\text{recon}}(\mathbf{y})] = \sum a_m(\mathbf{y}) \text{real}[d(\mathbf{k}_m)] + \sum b_m(\mathbf{y}) \text{imag}[d(\mathbf{k}_m)]$
(4) $\text{imag}[\rho_{p,\text{recon}}(\mathbf{y})] = \sum c_m(\mathbf{y}) \text{real}[d(\mathbf{k}_m)] + \sum d_m(\mathbf{y}) \text{imag}[d(\mathbf{k}_m)]$
(5) $\text{real}[\rho_{p,\text{recon}}(\mathbf{y})] = \int \text{real}[\rho_p(\mathbf{x})] \text{SRF}_y(\mathbf{x}) d\mathbf{x} + \int \text{imag}[\rho_p(\mathbf{x})] \text{IRF}_y(\mathbf{x}) d\mathbf{x} + \text{noise}(\mathbf{y})$
(6) $\text{SRF}_y(\mathbf{x}) = \sum a_m(\mathbf{y}) \cos[\varphi(\mathbf{x}) - 2\pi \mathbf{k}_m \cdot \mathbf{x}] + \sum b_m(\mathbf{y}) \sin[\varphi(\mathbf{x}) - 2\pi \mathbf{k}_m \cdot \mathbf{x}]$
(7) $\text{IRF}_y(\mathbf{x}) = \sum -a_m(\mathbf{y}) \sin[\varphi(\mathbf{x}) - 2\pi \mathbf{k}_m \cdot \mathbf{x}] + \sum b_m(\mathbf{y}) \cos[\varphi(\mathbf{x}) - 2\pi \mathbf{k}_m \cdot \mathbf{x}]$
(8) $\text{noise}(\mathbf{y}) = \sum a_m(\mathbf{y}) \text{real}[\eta_m] + \sum b_m(\mathbf{y}) \text{imag}[\eta_m]$ variance[noise(y)] = $(\sigma^2/2) \sum [a_m(\mathbf{y}) ^2 + b_m(\mathbf{y}) ^2]$

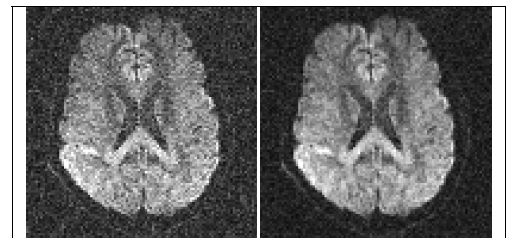


Figure 2. Standard PF (left) and smoothness-regularized (right) PF reconstructions of a 5/8th PF EPI acquisition. The smoothness regularized reconstruction utilized anatomical information derived from a sequence of coregistered diffusion-weighted images, as in [6].

The standard reconstruction has resolution on the order of $(2.17 \text{ mm})^2$ in-plane, while the regularized reconstruction has resolution on the order of $(2.36 \text{ mm})^2$ in-plane in smooth regions of the image, and 2 times the SNR of the standard reconstruction.